IEEE Access
Multidisciplinary | Rapid Review | Open Access Journal

Received June 13, 2019, accepted June 27, 2019, date of publication July 3, 2019, date of current version July 23, 2019.

Digital Object Identifier 10.1109/ACCESS.2019.2926541

Dynamics of Rogue Waves for a Generalized Inhomogeneous Third-Order Nonlinear Schrödinger Equation From the Heisenberg Ferromagnetic System

NI SONG AND HUI XUE
Department of Mathematics, School of Science, North University of China, Taiyuan 030051, China

Corresponding author: Ni Song (songni@nuc.edu.cn)

This work was supported in part by the National Natural Science Foundation of China (NNSFC) under Grant 11602232, in part by the Shanxi Natural Science Foundation (SNSF) under Grant 201801D221040 and Grant 201801D121158, and in part by the Fund for Shanxi under Grant 1331KIRT.

ABSTRACT In this paper, dynamics of the higher-order rogue waves for a generalized inhomogeneous third-order nonlinear Schrödinger equation is investigated by using the generalized Darboux transformation. Based on the Lax pair, the first-order to the third-order rogue wave solutions are derived through algebraic iteration starting from a seed solution. Nonlinear dynamical properties of rogue waves are analyzed on the basis of 3-D plots and density profiles. The new arrangement of the higher-order rogue waves is obtained. It is helpful to study the phenomenon of rogue waves in the Heisenberg ferromagnetic system.

INDEX TERMS Generalized Darboux transformation, Heisenberg ferromagnetic system, rogue waves, third-order nonlinear Schrödinger equation.

I. INTRODUCTION

Rogue waves, originated from the ocean dynamics, are short-peak waves with large amplitude above several tens of meters, which rise from the surrounding waves and have little relationship with the neighboring ones. They exist for a short time and disappear very quickly. Since Draper came up with the concept of rogue waves for the first time in 1965 [1], research on them has attracted considerable attention in various fields including the hydrodynamic surface [2], nonlinear fiber optics [3], Bose-Einstein condensates [4], atmospheric dynamics [5], plasma [6], capillary waves [7] and even finance [8]. Rogue waves are widely distributed in different sea areas of the world, which are very harmful to oil platforms, ship navigation, deep-sea fisheries and so on. It is dangerous and difficult to explore rogue waves in the ocean. The study on rogue waves, a hot topic in nonlinear fields, mainly focuses on the theoretical analysis [9], [10]. Nonlinear partial differential equations can be used to describe rogue waves. One of the most important models is nonlinear Schrödinger equation [11], [12]. In addition, Hirota equation [13], Sasa-Satsuma equation [14], Gross-Pitaevskii equation [15], Hirota-LPD equation [16], Hirota Maxwell-Bloch equation [17] and Fokas-Lenells [18] also play an important role in the study of rogue waves.

In recent years, many researchers have been studying nonlinear Schrödinger equation and made much progress. The generalized Darboux transformation (DT) [19] was proposed, which is an important tool to solve nonlinear Schrödinger equation. Song et al. constructed the higher-order rogue wave solutions for the inhomogeneous fourth-order nonlinear Schrödinger equation by using the generalized DT [20]. Chen *et al.* obtained the higher-order rational solutions and rogue wave solutions for a (2+1)-dimensional nonlinear Schrödinger equation [21]. Jia and Guo established the generalized N-fold DT and investigated the breathers and rogue waves for the nonlinear Schrödinger-Maxwell-Bloch equation [22]. Furthermore, Su *et al.* presented the generalized DT and rogue wave solutions for a generalized AB system [23]. Huang derived rational solitary wave and rogue wave solutions in coupled defocusing Hirota equation [24]. Yu et al. investigated localized analytical solutions and soliton stability for a nonlinear Gross-Pitaevskii equation with external potentials [25], [15].

The associate editor coordinating the review of this manuscript and approving it for publication was Shuai Liu.

 This work is licensed under a Creative Commons Attribution 4.0 License. For more information, see http://creativecommons.org/licenses/by/4.0/

Inspired by the pioneers' works, a generalized inhomogeneous third-order nonlinear Schrödinger equation will be discussed [26]

$$i\psi_t + i\varepsilon\psi_{xxx} + 6i\varepsilon|\psi|^2\psi_x + (f\psi)_{xx} - i(h\psi)_x + 2\psi\left(f|\psi|^2 + \int_{-\infty}^{x} f_x|\psi|^2 ds\right) = 0, \quad (1)$$

where $\psi(x,t)$ is a complex function with respect to the spatial coordinate x and the scaled time t. f and h represent the variation of the bilinear and biquadratic exchange interactions at different sites along the spin chain and

$$f = f_1 x + f_2, h = h_1 x + h_2, \quad (2)$$

f_i, h_i $(i = 1, 2)$ are real constants. ε is a small perturbation parameter. As for (1), it comes from the deformation of the Heisenberg ferromagnetic system by using prolongation structure theory in Minkowski space. With the help of the Hasimoto transformation, geometric equivalence relation is established between modified Heisenberg ferromagnetic spin chain equation and nonlinear Schrödinger equation in the [26]. In physics, ferromagnetic system plays a key role in information technology [27], [28] and nonlinear waves propagation [29]–[31]. There are many research results about Heisenberg ferromagnetic system [32]–[34]. However, little research about the rogue waves of (1) is reported in the existing literature. Therefore, it is expected to obtain some novel and different results to enrich the studies of rogue waves.

In the paper, the generalized DT is established for an inhomogeneous third-order nonlinear Schrödinger equation. The Nth-order rogue wave solutions are obtained in terms of a recursive formula. Starting from a seed solution, the first-order to the third-order rogue wave solutions are derived. Numerical simulations are carried out and dynamical characteristics are analyzed by selecting different parameters.

II. GENERALIZED DARBOUX TRANSFORMATION

In this section, we start from the 2×2 Lax pair ensuring the integrability of (1), which is given as follows

$$\Phi_x = U\Phi = \begin{pmatrix} -i\lambda & \psi \\ -\psi^* & i\lambda \end{pmatrix}\Phi, \quad (3)$$

$$\Phi_t = V\Phi = \begin{pmatrix} A & B \\ -B^* & -A \end{pmatrix}\Phi, \quad (4)$$

where

$$A = 2i\varepsilon\lambda|\psi|^2 - \varepsilon(\psi^*\psi_x - \psi\psi_x^*) - 4i\varepsilon\lambda^3 - 2if\lambda^2 + i\left(f|\psi|^2 + \int_{-\infty}^{x} f_x|\psi|^2 ds\right) - ih\lambda, \quad (5)$$

$$B = -2\varepsilon|\psi|^2\psi + 4\varepsilon\lambda^2\psi + 2i\varepsilon\lambda\psi_x - \varepsilon\psi_{xx} + i(f\psi)_x + 2f\lambda\psi + h\psi. \quad (6)$$

$\Phi = (\varphi, \phi)^T$ is an eigenfunction of the Lax pair, λ is a spectral parameter and the asterisk denotes the complex conjugation.

Basing on the procedure of DT for AKNS system in the reference [35], we can introduce a Darboux matrix T to satisfy

$$\Phi[1] = T\Phi. \quad (7)$$

Assume the Darboux matrix T meets the following condition

$$T = \lambda I - S, S = H\Lambda H^{-1}, \quad (8)$$

where

$$I = \begin{pmatrix} 1 & 0 \\ 0 & 1 \end{pmatrix}, \quad H = \begin{pmatrix} \varphi_1 & \phi_1^* \\ \phi_1 & -\varphi_1^* \end{pmatrix}, \quad \Lambda = \begin{pmatrix} \lambda_1 & 0 \\ 0 & \lambda_1^* \end{pmatrix}. \quad (9)$$

Let $\Phi_1 = (\varphi_1, \phi_1)^T$ be an eigenfunction of the Lax pair with a seed solution $\psi = \psi[0]$ and $\lambda = \lambda_1$. If different $\lambda = \lambda_k$ correspond to different eigenfunctions, the classical DT can be iterated successfully

$$\lambda = \lambda_k, \quad \Phi_k = (\varphi_k, \phi_k)^T \ (j = 1, 2, \ldots, N), \quad (10)$$

$$\Phi_N[N-1] = T[N-1]T[N-2]\cdots T[1]T[0]\Phi_N, \quad (11)$$

$$\psi[N] = \psi[0] - 2i\sum_{k=1}^{N}(\lambda_1 - \lambda_1^*) \times \frac{\varphi_k[k-1]\phi_k^*[k-1]}{|\varphi_k[k-1]|^2 + |\phi_k[k-1]|^2}, \quad (12)$$

$$T[k] = \lambda_{k+1}I - H[k-1]\Lambda[k]H[k-1]^{-1}, \quad (13)$$

where

$$H[k-1] = \begin{pmatrix} \varphi_k[k-1] & \phi_k^*[k-1] \\ \phi_k[k-1] & -\varphi_k^*[k-1] \end{pmatrix}, \quad (14)$$

$$\Lambda[k] = \begin{pmatrix} \lambda_k & 0 \\ 0 & \lambda_k^* \end{pmatrix}, \quad (15)$$

$$\Phi_k[k-1] = (T[k-1]T[k-2]\cdots T[1]T[0])|_{\lambda=\lambda_k}\Phi_k. \quad (16)$$

According to the above DT, the generalized DT of (1) is presented.

Taking the initial value in the following form

$$\Phi_1[0] = (\varphi_1[0], \phi_1[0])^T = (\varphi_1, \phi_1)^T = \Phi_1, \quad (17)$$

we assume that $\Psi = \Phi_1(\lambda_1, \eta)$ is a special solution of Lax pair at $\lambda = \lambda_1$, η is a small parameter. Using Maple, we can expand Ψ into the Taylor series at $\eta = 0$

$$\Psi = \Phi_1^{[0]} + \Phi_1^{[1]}\eta + \Phi_1^{[2]}\eta^2 + \cdots + \Phi_1^{[m]}\eta^m + o(\eta^m), \quad (18)$$

where

$$\Phi_1^{[j]} = \frac{1}{j!}\frac{\partial^j}{\partial\lambda^j}\Phi_1(\lambda)|_{\lambda=\lambda_1} \quad (j = 1, 2, \ldots, m). \quad (19)$$

It is easily verified that $\Phi_1^{[0]} = \Phi_1[0]$ is the special solution of Lax pair with a seed solution $\psi = \psi[0]$ and $\lambda = \lambda_1$. Hence, the zero-order generalized DT of (1) is defined as follows

$$\psi[1] = \psi[0] - 2i(\lambda_1 - \lambda_1^*)\frac{\varphi_1[0]\phi_1^*[0]}{|\varphi_1[0]|^2 + |\phi_1[0]|^2}. \quad (20)$$

Basing on the above process, the limit is calculated

$$\Phi_1[1] = \lim_{\eta\to 0}\frac{[T[1]|_{\lambda=\lambda_1+\eta}]\Psi}{\eta} = \lim_{\eta\to 0}\frac{[\eta + T[1]|_{\lambda=\lambda_1}]\Psi}{\eta} = \Phi_1^{[0]} + T_1[1](\lambda_1)\Phi_1^{[1]}. \quad (21)$$

Then, we derive the first-order generalized DT by iterating the zero-order one

$$\psi[2] = \psi[1] - 2i(\lambda_1 - \lambda_1^*)\frac{\varphi_1[1]\phi_1^*[1]}{|\varphi_1[1]|^2 + |\phi_1[1]|^2}. \quad (22)$$

Further, the $(N-1)$th-order generalized DT can be obtained

$$\Phi_1[N-1] = \Phi_1^{[0]} + \left[\sum_{l=1}^{N-1} T_1[l]\right]\Phi_1^{[1]} + \left[\sum_{l=1}^{N-1}\sum_{k>l}^{N-1} T_1[k]T_1[l]\right]\Phi_1^{[2]} + \cdots + [T_1[N-1]T_1[N-2]\cdots T_1[1]]\Phi_1^{[N-1]}, \quad (23)$$

$$\psi[N] = \psi[N-1] - 2i(\lambda_1 - \lambda_1^*)\frac{\varphi_1[N-1]\phi_1^*[N-1]}{|\varphi_1[N-1]|^2 + |\phi_1[N-1]|^2}, \quad (24)$$

$$T_1[k] = \lambda_1 I - H_1[k-1]\Lambda[1]H_1[k-1]^{-1}, \quad (25)$$

where

$$H_1[k-1] = \begin{pmatrix} \varphi_1[k-1] & \phi_1^*[k-1] \\ \phi_1[k-1] & -\varphi_1^*[k-1] \end{pmatrix}, \quad (26)$$

$$\Phi_1[k-1] = \begin{pmatrix} \varphi_1[k-1] \\ \phi_1[k-1] \end{pmatrix}. \quad (27)$$

From the above discussion, we gain the $(N-1)$th-order generalized DT, which is convenient to establish rogue wave solutions of (1) in the next section.

III. ROGUE WAVE SOLUTIONS

For the sake of simplicity, we assume that $f = 1$, $h = \frac{1}{6}$, which are independent of spatial coordinate x.

Starting with a seed solution $\psi[0] = ae^{i\theta}$, $\theta = kx + \omega t$, a and k are real constants and ω satisfies the nonlinear dispersion relation

$$\omega = \varepsilon k^3 - fk^2 - 6\varepsilon a^2 k + 2a^2 f + hk. \quad (28)$$

The corresponding eigenfunction $\Phi_1(\eta)$ of the Lax pair for linear spectral problem at $\lambda = \frac{k}{2} - ia + \eta^2$ is

$$\Phi_1(\eta) = \begin{pmatrix} (C_1 e^{\rho} + C_2 e^{-\rho})e^{\frac{i\theta}{2}} \\ (C_2 e^{\rho} + C_1 e^{-\rho})e^{-\frac{i\theta}{2}} \end{pmatrix}, \quad (29)$$

where

$$C_1 = \sqrt{-\mu + \frac{ik}{2} + i\lambda}, \quad C_2 = \sqrt{\mu + \frac{ik}{2} + i\lambda}, \quad (30)$$

$$\rho = \mu(x + \delta t + \Omega(\eta)), \quad (31)$$

$$\Omega(\eta) = \sum_{j=1}^{N}(a_j + ib_j)\eta^{2j} \quad (a_j, b_j \in R), \quad (32)$$

$$\delta = -2\varepsilon a^2 + 4\varepsilon\lambda^2 - 2\varepsilon\lambda k + \varepsilon k^2 - fk + 2f\lambda + h, \quad (33)$$

δ is a small parameter and $\Omega(\eta)$ is the separating function.

Let $a = 1, k = 0$, the function $\Phi_1(\eta)$ is expanded as Taylor series at $\eta = 0$

$$\Phi_1(\eta) = \Phi_1^{[0]} + \Phi_1^{[1]}\eta^2 + \Phi_1^{[2]}\eta^4 + \Phi_1^{[3]}\eta^6 + \cdots + \Phi_1^{[m]}\eta^{2m} + \cdots, \quad (34)$$

where

$$\Phi_1^{[0]} = \begin{pmatrix} \varphi_1^{[0]} \\ \phi_1^{[0]} \end{pmatrix}, \quad \Phi_1^{[1]} = \begin{pmatrix} \varphi_1^{[1]} \\ \phi_1^{[1]} \end{pmatrix}, \quad \Phi_1^{[2]} = \begin{pmatrix} \varphi_1^{[2]} \\ \phi_1^{[2]} \end{pmatrix}, \cdots. \quad (35)$$

Making use of Maple, we obtain corresponding coefficients of Taylor expansion

$$\varphi_1^{[0]} = 2\sqrt{a}e^{\frac{i\theta}{2}}, \quad \phi_1^{[0]} = 2\sqrt{a}e^{-\frac{i\theta}{2}}, \quad (36)$$

$$\varphi_1^{[1]} = \frac{1}{\sqrt{a}}\Big(\frac{1}{18}i(1296a^6\varepsilon^2t^2 + 864ia^5\varepsilon t^2 - 144a^4t^2 - 72a^4\varepsilon t^2 - 432a^4\varepsilon tx - 24ia^3t^2 - 144ia^3tx + a^2t^2 + 12a^2tx + 36a^2x^2 + 216a^3\varepsilon t + 72ia^2t - 6ta - 36ax + 9))e^{\frac{i\theta}{2}}, \quad (37)$$

$$\phi_1^{[1]} = \frac{1}{\sqrt{a}}\Big(\frac{1}{18}i(1296a^6\varepsilon^2t^2 + 864ia^5\varepsilon t^2 - 144a^4t^2 - 72a^4\varepsilon t^2 - 432a^4\varepsilon tx - 24ia^3t^2 - 144ia^3tx + a^2t^2 + 12a^2tx + 36a^2x^2 - 216a^3\varepsilon t - 72ia^2t + 6ta + 36ax + 9))e^{-\frac{i\theta}{2}}. \quad (38)$$

$\varphi_1^{[2]}$ and $\phi_1^{[2]}$ are given in the Appendix A.

We expect to construct rogue wave solutions using the $(N-1)$th-order iterative formulas and coefficients of Taylor expansion.

A. FIRST-ORDER ROGUE WAVE SOLUTION

Actually, it could be easily verified that $\Phi_1^{[0]}$ is the solution of Lax pair with a seed solution $\psi[0] = e^{i\theta}$ and $\lambda = -i$. Substituting $\Phi_1^{[0]}$, $\psi[0] = e^{i\theta}$ and $\lambda = -i$ into (20), we can obtain a trival solution $\psi[1]$ of (1)

$$\psi[1] = -e^{i\theta}, \quad T_1[1] = \begin{pmatrix} -i & ie^{i\theta} \\ ie^{-i\theta} & -i \end{pmatrix}. \quad (39)$$

Then we work out the following limit

$$\Phi_1[1] = \lim_{\eta\to 0}\frac{[T[1]|_{\lambda=\lambda_1+\eta}]\Psi}{\eta} = \lim_{\eta\to 0}\frac{[\eta + T[1]|_{\lambda=\lambda_1}]\Psi}{\eta} = \Phi_1^{[0]} + T_1[1](\lambda_1)\Phi_1^{[1]}, \quad (40)$$

the first-order rogue wave solution of (1) is obtained

$$\psi[2] = \psi[1] - 2i(\lambda_1 - \lambda_1^*)\frac{\varphi_1[1]\phi_1^*[1]}{|\varphi_1[1]|^2 + |\phi_1[1]|^2} = \left(\frac{F}{G}\right)e^{i\theta}, \quad (41)$$

where

$$F = 1296\varepsilon^2t^2 - 72\varepsilon t^2 - 432\varepsilon tx - 144it + 145t^2 + 12tx + 36x^2 - 27, \quad (42)$$

$$G = 1296\varepsilon^2t^2 - 72\varepsilon t^2 - 432\varepsilon tx + 145t^2 + 12tx + 36x^2 + 9, \quad (43)$$

$$\varphi_1[1] = \frac{2}{3}\sqrt{a}(36a^3\varepsilon t + 12ia^2t - ta - 6ax + 3)e^{\frac{i\theta}{2}}, \quad (44)$$

$$\phi_1[1] = -\frac{2}{3}\sqrt{a}(36a^3\varepsilon t + 12ia^2t - ta - 6ax - 3)e^{-\frac{i\theta}{2}}. \quad (45)$$

There is merely a free parameter ε in the first-order rogue wave solution. Setting $\varepsilon = 0$, equation (1) is changed into nonlinear Schrödinger equation with the first partial derivative term. Three-dimensional plot and density profile are shown in Figure 1. It is the fundamental form of the first-order rogue wave. The maximum amplitude is 3, which occurs at $t = 0, x = 0$. The amplitude suddenly increases at the center and quickly disappears. In Figure 2, we have $\varepsilon = 0.1$. There is a little incline as the small perturbation parameter ε changes, which has no influence on the structure of rogue waves. In the following discussion, we could assume $\varepsilon = 0$.

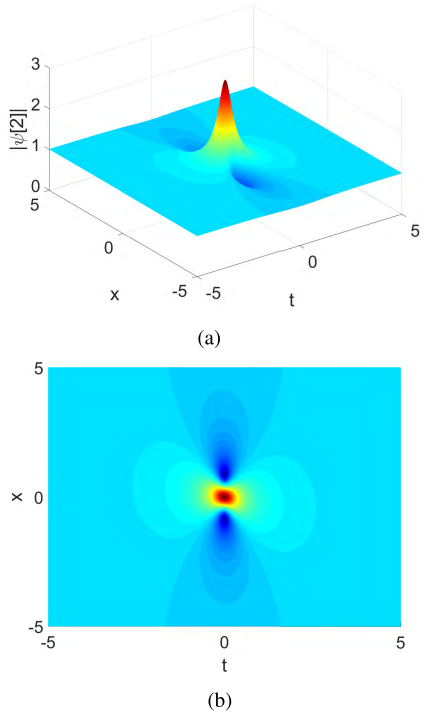

FIGURE 1. The first-order rogue wave with $\varepsilon = 0$.

B. SECOND-ORDER ROGUE WAVE SOLUTION

Putting more attention on the limitation

$$\Phi_1[2] = \lim_{\eta\to 0}\frac{[\eta + T[2]|_{\lambda=\lambda_1}][\eta + T[1]|_{\lambda=\lambda_1}]\Psi}{\eta^2} = \Phi_1^{[0]} + (T_1[2](\lambda_1) + T_1[1](\lambda_1))\Phi_1^{[1]} + T_1[2](\lambda_1)T_1[1](\lambda_1)\Phi_1^{[2]}, \quad (46)$$

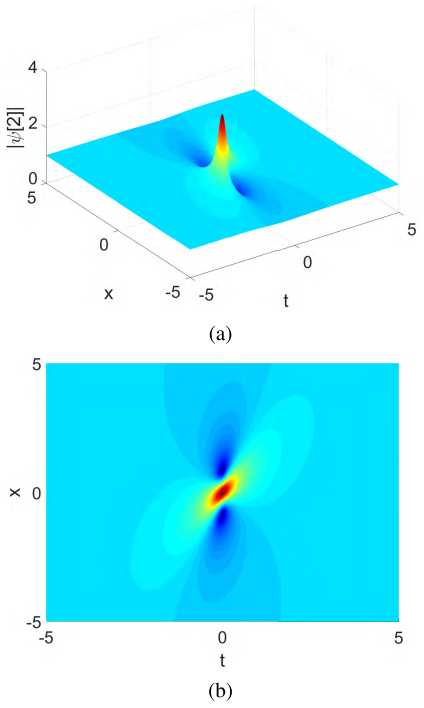

FIGURE 2. The first-order rogue wave with $\varepsilon = 0.1$.

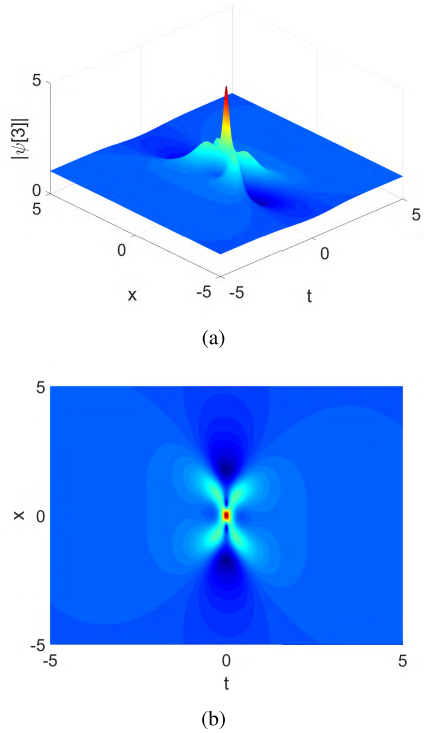

FIGURE 3. The second-order rogue wave with $a_1 = b_1 = 0$.

where

$$\Phi_1[2] = \begin{pmatrix}\varphi_1[2]\\ \phi_1[2]\end{pmatrix}. \quad (47)$$

$T_1[2]$ is worked out by Maple. $\varphi_1[2]$ and $\phi_1[2]$ are presented in the Appendix B. Further, the second-order rogue wave

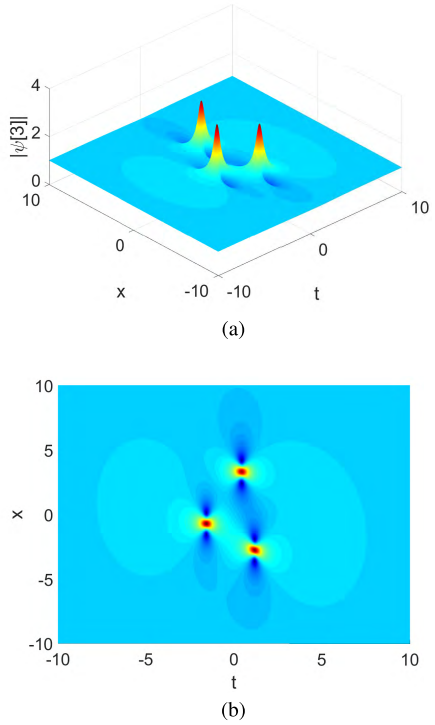

FIGURE 4. The second-order rogue wave with $a_1 = b_1 = 20$.

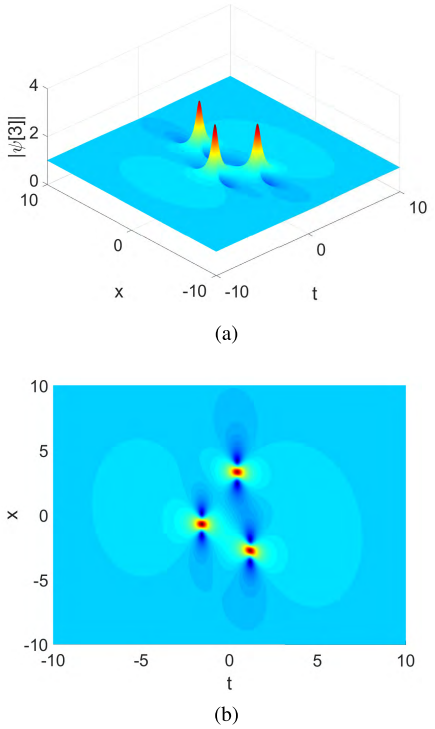

FIGURE 5. The second-order rogue wave with $a_1 = b_1 = 200$.

solution of (1) can be obtained

$$\psi[3] = \psi[2] - 4\frac{\varphi_1[2]\phi_1^*[2]}{|\varphi_1[2]|^2 + |\phi_1[2]|^2}. \tag{48}$$

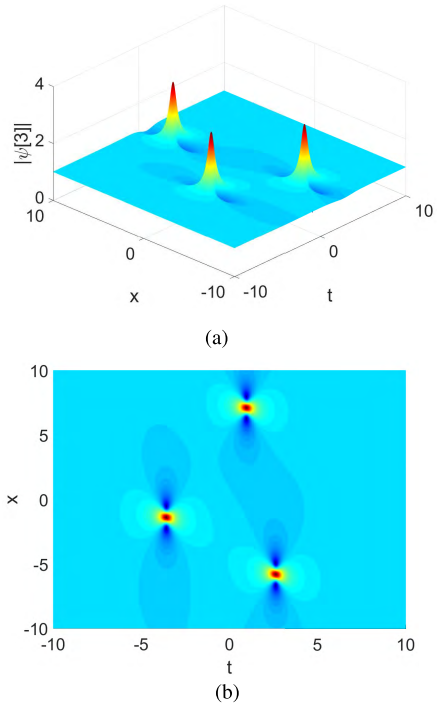

FIGURE 6. The third-order rogue wave with $a_1 = a_2 = 0$, $b_1 = b_2 = 0$.

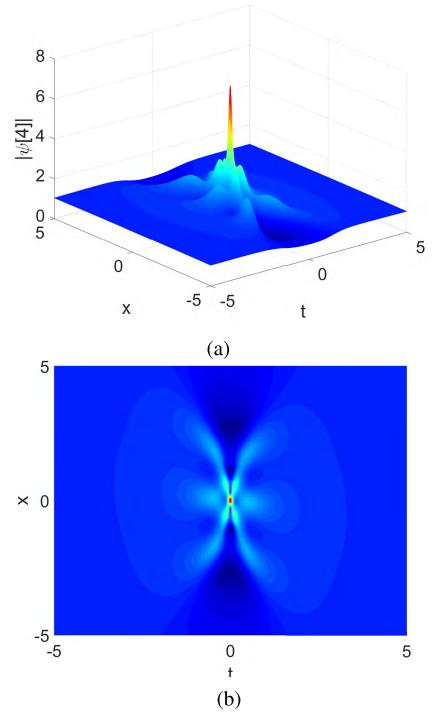

FIGURE 7. The third-order rogue wave with $a_1 = a_2 = 60$, $b_1 = b_2 = 0$.

There are three parameters ε, a_1 and b_1 in the solution $\psi[3]$. When the parameters $a_1 = b_1 = 0$, the plots of the solution $\psi[3]$ are exhibited in Figure 3. It is the fundamental pattern of the second-order rogue wave and the maximum amplitude of $|\psi[3]|$ is 5. A bigger rogue wave lies in the

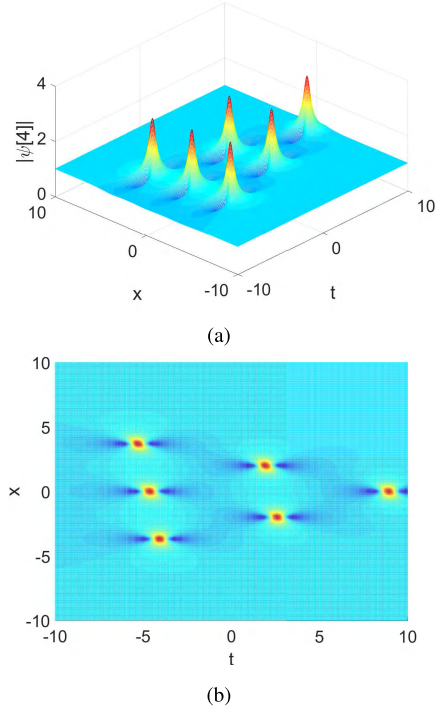

FIGURE 8. The third-order rogue wave with $a1 = a2 = 0, b1 = 0, b2 = 80$.

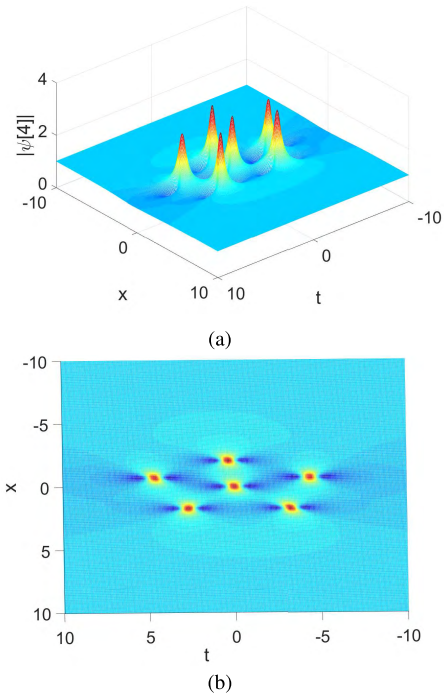

FIGURE 9. The third-order rogue wave with $a_1 = a_2 = 0, b_1 = 0, b_2 = 200$.

center and four smaller ones are distributed symmetrically on both sides.

Then, we will put the separating function into consideration. Suppose $a_1 = b_1 = 20$, three-dimensional plot and density profile are illustrated in Figure 4. It is shown that the second-order rogue waves are divided into three first-order ones, which have a structure of an isosceles triangle. Increasing the values $a_1 = b_1 = 200$, the corresponding plots of $\psi[3]$ are displayed in Figure 5. Clearly, three first-order rogue waves are separated completely.

C. THIRD-ORDER ROGUE WAVE SOLUTION

Taking the following limit into account

$$\begin{aligned}\Phi_1[3] &= \lim_{\eta\to 0}\frac{[\eta+T[3]|_{\lambda=\lambda_1}][\eta+T[2]|_{\lambda=\lambda_1}][\eta+T[1]|_{\lambda=\lambda_1}]\Psi}{\eta^3}\\ &= \Phi_1^{[0]} + (T_1[3](\lambda_1) + T_1[2](\lambda_1) + T_1[1](\lambda_1))\Phi_1^{[1]}\\ &\quad + (T_1[2](\lambda_1)T_1[1](\lambda_1) + T_1[3](\lambda_1)T_1[1](\lambda_1)\\ &\quad + T_1[3](\lambda_1)T_1[2](\lambda_1))\Phi_1^{[2]}\\ &\quad + T_1[3](\lambda_1)T_1[2](\lambda_1)T_1[1](\lambda_1)\Phi_1^{[3]}, \end{aligned} \tag{49}$$

where $T_1[3]$ and $\Phi_1[3]$ can be calculated by Maple, which are neglected because of their cumbersome forms. Hence, the third-order rogue wave solution is derived

$$\psi[4] = \psi[3] - 4\frac{\varphi_1[3]\phi_1^*[3]}{|\varphi_1[3]|^2 + |\phi_1[3]|^2}. \tag{50}$$

There are five free parameters ε, a_1, b_1, a_2, and b_2 in the solution $\psi[4]$. Suppose the parameters $a_1 = a_2 = 0$ and $b_1 = b_2 = 0$, three-dimensional plot and density profile are displayed in Figure 6. It is a fundamental pattern of the third-order rogue wave and the maximum amplitude is 7.

Changing the parameters as $a_1 = a_2 = 60$, three-dimensional plot and density profile are depicted in Figure 7. It is observed that the third-order rogue wave are made up of six first-order rogue waves, which form an equilateral triangle.

Assuming $a_1 = a_2 = 0$, $b_1 = 0$ and $b_2 = 80$, the corresponding plots are shown in Figure 8. The six first-order rogue waves array an isosceles triangle. Furthermore, adjusting the parameter $b_2 = 200$ and other parameters being the same, three-dimensional plot and density profile are illustrated in Figure 9. It is clear that six first-order rogue waves are arranged in pairs and have a form of "W". A pair of them is in the center, other two pairs are symmetrically distributed on both sides.

Setting $a_1 = 0$, $a_2 = 200$ and $b_1 = b_2 = 0$, three-dimensional plot and density profile are demonstrated in Figure 10. It can be seen that different configuration of rogue waves appears, which has a ring structure with six peaks.

It is remarkable to note that Figure 9 is a new structure of the third-order rogue waves, which enrich the studies of the nonlinear Schrödinger equation. It is guessed that there are more novel structures of the higher-order rogue wave solution.

IV. CONCLUSIONS

In this paper, we investigated the higher-order rogue waves of a generalized inhomogeneous third-order nonlinear Schrödinger equation. Based on the classical DT, the general-

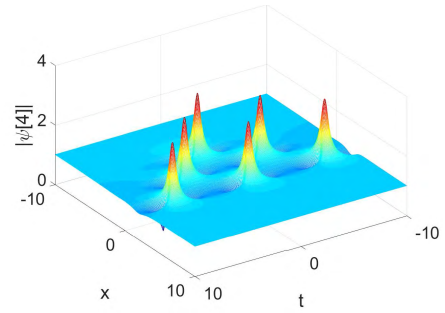

(a)

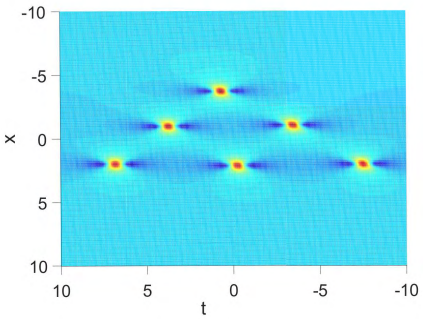

(b)

FIGURE 10. The third-order rogue wave with $a1 = 0$, $a2 = 200$, $b1 = b2 = 0$.

ized DT is deduced by using Taylor expansion and limit procedures. The first-order to the third-order rogue wave solutions are constructed through the algebraic iteration starting from a seed solution. Nonlinear dynamic behaviors of rogue waves are analyzed with numerical simulations. We hope the results will be useful to come up with new ideas in nonlinear optics theory, experiment and engineering application.

APPENDIX A

$$\begin{aligned}\varphi_1^{[2]} = (&-\frac{1}{3888}\frac{1}{a^{3/2}}(-243 + 19440ia^2t - 9072ia^3t^2\\ &+ 7776ia^2a_1 - 194400a^4\varepsilon tx - 15552a^6\varepsilon t^2x^2\\ &- 31104a^6\varepsilon tx^3 + 15552a^5\varepsilon t^2x + 46656a^5\varepsilon tx^2\\ &- 93312a^5\varepsilon tb_1 - 15552ia^3xa_1 + 373248a^8\varepsilon t^3x\\ &-1119744a^{10}\varepsilon^3t^3x+93312a^8\varepsilon^2t^3x+279936a^8\varepsilon^2t^2x^2\\ &- 279936a^7\varepsilon^2t^2x - 2592a^6\varepsilon t^3x + 2239488ia^{11}\varepsilon^3t^4\\ &- 186624ia^9\varepsilon^2t^4 - 2592ia^3ta_1 - 54432ia^3tx\\ &- 31104ia^4tb_1 + 15552ia^4tx^2 + 5184ia^4t^2x\\ &+ 575424ia^5\varepsilon t^2 - 324ta - 186624ia^6\varepsilon t^2x\\ &+ 93312ia^5\varepsilon ta_1 - 864ia^5t^3x - 248832ia^9\varepsilon t^4\\ &+ 559872ia^8\varepsilon^2t^3+20736a^8t^4+5184a^5t^3-864a^6t^4\\ &+ 1296a^4x^4 - 12a^3t^3 - 2592a^3x^3 - 7776a^2b_1\\ &- 85536a^4t^2 + 162a^2t^2 + 5832a^2x^2 - 1944ax\\ &+ a^4t^4 + 5184ia^7\varepsilon t^4 + 41472ia^7t^3x - 31104ia^6\varepsilon t^3\\ &- 5184ia^5t^2x^2 + 432ia^4t^3 + 186624ia^7\varepsilon t^2x^2\\ &+ 62208ia^7\varepsilon t^3x - 1119744ia^9\varepsilon^2t^3x - 48ia^5t^4\\ &- 20736ia^6t^3 + 6912ia^7t^4 - 10368ia^5tx^3\\ &+ 7776a^8\varepsilon^2t^4 - 144a^6\varepsilon t^4 - 46656a^7\varepsilon^2t^3\\ &+ 24a^4t^3x + 559872a^9\varepsilon^3t^3 + 1296a^5\varepsilon t^3\\ &+ 1679616a^{12}\varepsilon^4t^4 + 864a^4tx^3 + 216a^4t^2x^2\\ &-186624a^{10}\varepsilon^3t^4-216a^3t^2x-1296a^3tx^2+2592a^3tb_1\\ &+ 15552a^3xb_1 - 1119744a^{10}\varepsilon^2t^4 - 186624a^7\varepsilon t^3\\ &+ 62208a^8\varepsilon t^4 + 31104a^5t^2x - 10368a^6t^3x\\ &- 31104a^6t^2x^2 - 31104a^4ta_1 + 1944a^2tx\\ &+ 956448a^6\varepsilon^2t^2 - 32400a^4\varepsilon t^2 + 73872a^3\varepsilon t))e^{\frac{i\theta}{2}},\end{aligned}$$

$$\begin{aligned}\phi_1^{[2]} = (&-\frac{1}{3888}\frac{1}{a^{3/2}}(-243 - 19440ia^2t - 9072ia^3t^2\\ &- 7776ia^2a_1 - 194400a^4\varepsilon tx - 15552a^6\varepsilon t^2x^2\\ &- 31104a^6\varepsilon tx^3 - 15552a^5\varepsilon t^2x - 46656a^5\varepsilon tx^2\\ &- 93312a^5\varepsilon tb_1 - 15552ia^3xa_1 + 373248a^8\varepsilon t^3x\\ &-1119744a^{10}\varepsilon^3t^3x+93312a^8\varepsilon^2t^3x+279936a^8\varepsilon^2t^2x^2\\ &+ 279936a^7\varepsilon^2t^2x - 2592a^6\varepsilon t^3x + 2239488ia^{11}\varepsilon^3t^4\\ &- 186624ia^9\varepsilon^2t^4 - 2592ia^3ta_1 - 54432ia^3tx\\ &- 31104ia^4tb_1 - 15552ia^4tx^2 - 5184ia^4t^2x\\ &+ 575424ia^5\varepsilon t^2 + 324ta + 186624ia^6\varepsilon t^2x\\ &+ 93312ia^5\varepsilon ta_1\\ &- 864ia^5t^3x - 248832ia^9\varepsilon t^4 - 559872ia^8\varepsilon^2t^3\\ &+20736a^8t^4-5184a^5t^3-864a^6t^4+1296a^4x^4+12a^3t^3\\ &+ 2592a^3x^3 + 7776a^2b_1 - 85536a^4t^2 + 162a^2t^2\\ &+ 5832a^2x^2 + 1944ax + a^4t^4 + 5184ia^7\varepsilon t^4\\ &+ 41472ia^7t^3x + 31104ia^6\varepsilon t^3 - 5184ia^5t^2x^2\\ &- 432ia^4t^3 + 186624ia^7\varepsilon t^2x^2 + 62208ia^7\varepsilon t^3x\\ &- 1119744ia^9\varepsilon^2t^3x - 48ia^5t^4 + 20736ia^6t^3\\ &+ 6912ia^7t^4-10368ia^5tx^3+7776a^8\varepsilon^2t^4-144a^6\varepsilon t^4\\ &+ 46656a^7\varepsilon^2t^3+24a^4t^3x-559872a^9\varepsilon^3t^3-1296a^5\varepsilon t^3\\ &+ 1679616a^{12}\varepsilon^4t^4 + 864a^4tx^3 + 216a^4t^2x^2\\ &- 186624a^{10}\varepsilon^3t^4\\ &+ 216a^3t^2x+1296a^3tx^2 + 2592a^3tb_1 + 15552a^3xb_1\\ &-1119744a^{10}\varepsilon^2t^4+186624a^7\varepsilon t^3+62208a^8\varepsilon t^4\\ &- 31104a^5t^2x - 10368a^6t^3x - 31104a^6t^2x^2\\ &- 31104a^4ta_1\\ &+ 1944a^2tx + 956448a^6\varepsilon^2t^2 - 32400a^4\varepsilon t^2\\ &- 73872a^3\varepsilon t))e^{-\frac{i\theta}{2}}.\end{aligned}$$

APPENDIX B

$$\begin{aligned}&\varphi_1[2]\\ &= \frac{2}{27}\frac{1}{\Delta}\sqrt{a}(243 - 11664ia^5\varepsilon ta_1 + 93312ia^7\varepsilon t^2x^2\\ &+ 31104ia^7\varepsilon t^3x - 3456ia^7t^4 + 20736ia^6t^3\\ &- 24ia^5t^4 - 559872ia^9\varepsilon^2t^3x - 5184ia^5tx^3\\ &- 2592ia^5t^2x^2 + a^4t^4 - 2592a^5t^3 - 20736a^8t^4\end{aligned}$$

$$
\begin{aligned}
&-972ax+1296a^4x^4-972a^2b_1-6a^3t^3\\
&-1296a^3x^3-7776a^4t^2-162ta+2592ia^7\varepsilon t^4\\
&+23328a^5\varepsilon tx^2+15552a^4\varepsilon tx-2592a^6\varepsilon t^3x\\
&-15552a^6\varepsilon t^2x^2+93312a^8\varepsilon^2t^3x+279936a^8\varepsilon^2t^2x^2\\
&-1119744a^{10}\varepsilon^3t^3x-31104a^6\varepsilon tx^3+11664a^5\varepsilon tb_1\\
&-139968a^7\varepsilon^2t^2x+7776a^5\varepsilon t^2x-20736ia^7t^3x\\
&-432ia^5t^3x+93312a^7\varepsilon t^3-186624a^{10}\varepsilon^3t^4\\
&+864a^4tx^3-93312a^6\varepsilon^2t^2-144a^6\varepsilon t^4\\
&+648a^5\varepsilon t^3-324a^3tb_1-3888a^4ta_1+1679616a^{12}\varepsilon^4t^4\\
&+279936a^9\varepsilon^3t^3+2592a^4\varepsilon t^2+13608a^3\varepsilon t\\
&+216a^4t^2x^2-23328a^7\varepsilon^2t^3+24a^4t^3x+7776a^8\varepsilon^2t^4\\
&-15552a^5t^2x-1944a^3xb_1-648a^3tx^2-108a^3t^2x\\
&+648ia^3t^2+3888ia^2t+7776ia^5\varepsilon t^2-3888ia^4tb_1\\
&+3888ia^3tx+324ia^3ta_1+1944ia^3xa_1\\
&+1119744ia^{11}\varepsilon^3t^4-93312ia^9\varepsilon^2t^4+124416ia^9\varepsilon t^4\\
&+972ia^2a_1)e^{\frac{i\theta}{2}},
\end{aligned}
$$

$$
\begin{aligned}
\phi_1[2]&=\frac{2}{27}\frac{1}{\Delta}\sqrt{a}(243-11664ia^5\varepsilon ta_1+93312ia^7\varepsilon t^2x^2\\
&+31104ia^7\varepsilon t^3x-3456ia^7t^4-20736ia^6t^3\\
&-24ia^5t^4-559872ia^9\varepsilon^2t^3x-5184ia^5tx^3\\
&-2592ia^5t^2x^2+a^4t^4+2592a^5t^3-20736a^8t^4\\
&+972ax+1296a^4x^4+972a^2b_1+6a^3t^3\\
&+1296a^3x^3-7776a^4t^2+162ta+2592ia^7\varepsilon t^4\\
&-23328a^5\varepsilon tx^2+15552a^4\varepsilon tx-2592a^6\varepsilon t^3x\\
&-15552a^6\varepsilon t^2x^2+93312a^8\varepsilon^2t^3x+279936a^8\varepsilon^2t^2x^2\\
&-1119744a^{10}\varepsilon^3t^3x-31104a^6\varepsilon tx^3+11664a^5\varepsilon tb_1\\
&+139968a^7\varepsilon^2t^2x-7776a^5\varepsilon t^2x-20736ia^7t^3x\\
&-432ia^5t^3x-93312a^7\varepsilon t^3-186624a^{10}\varepsilon^3t^4\\
&+864a^4tx^3-93312a^6\varepsilon^2t^2-144a^6\varepsilon t^4\\
&-648a^5\varepsilon t^3-324a^3tb_1-3888a^4ta_1+1679616a^{12}\varepsilon^4t^4\\
&-279936a^9\varepsilon^3t^3+2592a^4\varepsilon t^2-13608a^3\varepsilon t\\
&+216a^4t^2x^2+23328a^7\varepsilon^2t^3+24a^4t^3x+7776a^8\varepsilon^2t^4\\
&+15552a^5t^2x-1944a^3xb_1+648a^3tx^2+108a^3t^2x\\
&+648ia^3t^2-3888ia^2t+7776ia^5\varepsilon t^2-3888ia^4tb_1\\
&+3888ia^3tx+324ia^3ta_1+1944ia^3xa_1\\
&+1119744ia^{11}\varepsilon^3t^4-93312ia^9\varepsilon^2t^4+124416ia^9\varepsilon t^4\\
&-972ia^2a_1)e^{-\frac{i\theta}{2}},
\end{aligned}
$$

$$
\begin{aligned}
\Delta=\;&1296a^6\varepsilon^2t^2-72a^4\varepsilon t^2-432a^4\varepsilon tx+144a^4t^2+a^2t^2\\
&+12a^2tx+36a^2x^2+9.
\end{aligned}
$$

REFERENCES

[1] L. Draper, "Freak wave," *Mar. Observer*, vol. 35, no. 2, pp. 193–195, 1965.

[2] I. Pelinovsky and C. Kharif, *Extreme Ocean Waves*. Berlin, Germany: Springer, 2008.

[3] D. R. Solli, C. Ropers, P. Koonath, and B. Jalali, "Optical rogue waves," *Nature*, vol. 450, pp. 1054–1057, Dec. 2007.

[4] Y. V. Bludov, V. V. Konotop, and N. Akhmediev, "Matter rogue waves," *Phys. Lett. A*, vol. 80, Sep. 2009, Art. no. 033610.

[5] L. Stenflo and M. Marklund, "Rogue waves in the atmosphere," *J. Plasma Phys.*, vol. 76, nos. 3–4, pp. 293–295, Jan. 2010.

[6] A. S. Bains, M. Tribeche, N. S. Saini, and T. S. Gill, "Modulation instability and rogue wave structures of positron-acoustic waves in q-nonextensive plasmas," *Phys. A, Stat. Mech. Appl.*, vol. 466, pp. 111–119, Jan. 2017.

[7] M. Shats, H. Punzmann, and H. Xia, "Capillary rogue waves," *Phys. Rev. Lett.*, vol. 104, Mar. 2010, Art. no. 104503.

[8] Z. Y. Yan, "Financial rogue waves," *Commun. Theor. Phys.*, vol. 54, no. 5, p. 947, Nov. 2010.

[9] Y.-L. Ma and B.-Q. Li, "Analytic rogue wave solutions for a generalized fourth-order Boussinesq equation in fluid mechanics," *Math. Methods Appl. Sci.*, vol. 42, no. 1, pp. 39–48, Jan. 2019.

[10] Y.-L. Ma and B.-Q. Li, "Interactions between soliton and rogue wave for a (2+1)-dimensional generalized breaking soliton system: Hidden rogue wave and hidden soliton," *Comput. Math. Appl.*, vol. 78, no. 3, pp. 827–839, Aug. 2019.

[11] J.-G. Caputo and A. I. Maimistov, "Unidirectional propagation of an ultrashort electromagnetic pulse in a resonant medium with high frequency Stark shift," *Phys. Lett. A*, vol. 296, no. 1, pp. 34–42, Apr. 2002.

[12] A. Ankiewicz, D. J. Kedziora, A. Chowdury, U. Bandelow, and N. Akhmediev, "Infinite hierarchy of nonlinear Schrödinger equations and their solutions," *Phys. Rev. E, Stat. Phys. Plasmas Fluids Relat. Interdiscip. Top.*, vol. 93, no. 1, Jan. 2016, Art. no. 012206.

[13] A. Ankiewicz, J. M. Soto-Crespo, and N. Akhmediev, "Rogue waves and rational solutions of the Hirota equation," *Phys. Rev. E, Stat. Phys. Plasmas Fluids Relat. Interdiscip. Top.*, vol. 81, no. 4, Apr. 2010, Art. no. 046602.

[14] U. Bandelow and N. Akhmediev, "Persistence of rogue waves in extended nonlinear Schrödinger equations: Integrable Sasa–Satsuma case," *Phys. Lett. A*, vol. 376, no. 18, pp. 1558–1561, Apr. 2012.

[15] F. J. Yu and L. Li, "Inverse scattering transformation and soliton stability for a nonlinear Gross–Pitaevskii equation with external potentials," *Appl. Math. Lett.*, vol. 91, pp. 41–47, May 2019.

[16] F. Yu, "Nonautonomous rogue waves and 'catch' dynamics for the combined Hirota–LPD equation with variable coefficients," *Commun. Nonlinear Sci. Numer. Simul.*, vol. 34, pp. 142–153, May 2016.

[17] C. Li, J. He, and K. Porsezian, "Rogue waves of the Hirota and the Maxwell-Bloch equations," *Phys. Rev. E, Stat. Phys. Plasmas Fluids Relat. Interdiscip. Top.*, vol. 87, Jan. 2013, Art. no. 012913.

[18] J. Lenells, "Dressing for a novel integrable generalization of the nonlinear Schrödinger equation," *J. Nonlinear Sci.*, vol. 20, no. 6, pp. 709–722, Dec. 2010.

[19] B. L. Guo, L. M. Ling, and Q. P. Liu, "Nonlinear Schrödinger equation: Generalized Darboux transformation and rogue wave solutions," *Phys. Rev. E, Stat. Phys. Plasmas Fluids Relat. Interdiscip. Top.*, vol. 85, no. 2, Feb. 2012, Art. no. 026607.

[20] N. Song, W. Zhang, and M. H. Yao, "Complex nonlinearities of rogue waves in generalized inhomogeneous higher-order nonlinear Schrödinger equation," *Nonlinear Dyn.*, vol. 82, nos. 1–2, pp. 489–500, Oct. 2015.

[21] M. Chen, B. Li, and Y.-X. Yu, "Darboux transformations, higher-order rational solitons and rogue wave solutions for a (2+1)-dimensional nonlinear Schrödinger equation," *Commun. Theor. Phys.*, vol. 71, no. 1, pp. 27–36, Jan. 2019.

[22] R.-R. Jia and R. Guo, "Breather and rogue wave solutions for the (2+1)-dimensional nonlinear Schrödinger–Maxwell–Bloch equation," *Appl. Math. Lett.*, vol. 93, pp. 117–123, Jul. 2019.

[23] J.-J. Su, Y.-T. Gao, and C.-C. Ding, "Darboux transformations and rogue wave solutions of a generalized AB system for the geophysical flows," *Appl. Math. Lett.*, vol. 88, pp. 201–208, Feb. 2018.

[24] X. Huang, "Rational solitary wave and rogue wave solutions in coupled defocusing Hirota equation," *Phys. Lett. A*, vol. 380, nos. 25–26, pp. 2136–2141, Jun. 2016.

[25] F. J. Yu, "Localized analytical solutions and numerically stabilities of generalized Gross–Pitaevskii (GP(p, q)) equation with specific external potentials," *Appl. Math. Lett.*, vol. 85, pp. 1–7, Nov. 2018.

[26] F. Zhang, *The Prolongation Structure of Anisotropic Modified Heisenberg Ferromagnet Equation*, (Chinese). Beijing, China: Capital Normal Univ., 2008.

[27] M. Tanaka, S. Ohya, and P. N. Hai, "Recent progress in III-V based ferromagnetic semiconductors: Band structure, Fermi level, and tunneling transport," *Appl. Phys. Rev.*, vol. 1, Jan. 2014, Art. no. 011102.

[28] L. Kavitha, E. Parasuraman, D. Gopi, and S. Bhuvaneswari, "Propagation of electromagnetic solitons in an antiferromagnetic spinladder medium," *J. Electromagn. Waves Appl.*, vol. 30, no. 6, pp. 740–766, Apr. 2016.

[29] H. T. Tchokouansi, V. K. Kuetche, and T. C. Kofane, "On the propagation of solitons in ferrites: The inverse scattering approach," *Chaos, Solitons Fractals*, vol. 86, pp. 64–74, May 2016.
[30] B. Q. Li and Y. L. Ma, "Loop-like periodic waves and solitons to the Kraenkel–Manna–Merle system in ferrites," *J. Electromagn. Waves Appl.*, vol. 32, pp. 1275–1286, Jan. 2018.
[31] B.-Q. Li and Y.-L. Ma, "Characteristics of rogue waves for a (2+1)-dimensional Heisenberg ferromagnetic spin chain system," *J. Magn. Magn. Mater.*, vol. 474, pp. 537–543, Mar. 2019.
[32] D.-W. Zuo, Y.-T. Gao, L. Xue, Y.-H. Sun, and Y.-J. Feng, "Rogue-wave interaction for the Heisenberg ferromagnetism system," *Phys. Scripta*, vol. 90, no. 3, Feb. 2015, Art. no. 035201.
[33] Y.-L. Ma, B.-Q. Li, and Y.-Y. Fu, "A series of the solutions for the Heisenberg ferromagnetic spin chain equation," *Math. Methods Appl. Sci.*, vol. 41, no. 9, pp. 3316–3322, Jun. 2018.
[34] B. Q. Li and Y. L. Ma, "Lax pair, Darboux transformation and Nth-order rogue wave solutions for a (2+1)-dimensional Heisenberg ferromagnetic spin chain equation," *Comput. Math. Appl.*, vol. 77, no. 2, pp. 514–524, Jan. 2019.
[35] L. Zhou, "Darboux transformation for the nonisospectral AKNS system," *Phys. Lett. A*, vol. 345, nos. 4–6, pp. 314–322, Oct. 2005.

NI SONG was born in Shanxi, China, in 1979. She received the Ph.D. degree from the Beijing University of Technology, Beijing, China, in 2015. She is currently an Associate Professor and a Master Tutor with the Department of Mathematics, North University of China, Shanxi. Her research interests include dynamics systems and nonlinear analysis fields.

HUI XUE was born in Shanxi, China, in 1994. She received the bachelor's degree from the Department of Mathematics, Taiyuan Normal University, Shanxi. She is currently pursuing the master's degree with the Department of Mathematics, School of Science, North University of China, Shanxi. Her research interest includes nonlinear analysis and application.